Robotica (2002) volume 20, pp. 23–31. © 2002 Cambridge University Press
DOI: 10.1017/S0263574701003642 Printed in the United Kingdom

A neural model for visual-tactile-motor integration in robotic reaching and grasping tasks

J. López-Coronado†, J.L. Pedreño-Molina*, A. Guerrero-González† and P. Gorce‡

(Received in Final Form: May 30, 2001)

SUMMARY

This paper presents a neural model to solve the visual-tactile-motor coordination problem in robotic applications. The proposed neural controller is based on the VAMC (Vector Associative Map) model. This algorithm is based on the human biological system and has the ability of learning the mapping that establishes the relationship between the spatial and the motor coordinates. These spatial inputs are composed of visual and force parameters. The LINCE stereohead carries out a visual detection process, detecting the positions of the object and of the manipulator. The artificial tactile skins placed over the two fingers of the gripper measure the force distribution when an object is touched. The neural controller has been implemented for robotic operations of reaching and object grasping. The reaching process is fed back in order to minimize the Difference Vector (DV) between the visual projections of the object and the manipulator. The stable grasping task processes the force distribution maps detected in the contact with the two surfaces of the gripper, in order to direct the object into the robotic fingers. Experimental results have demonstrated the robustness of the model and the accuracy of the final pick-and-place process.

KEYWORDS: Visual-tactile-motor control; Neural controller; Tactile skins; Grasp stability; Learning; Reaching.

1. INTRODUCTION

One of the first works found in the literature about the control of robots using external sensorial information was presented in 1979 by Hill and Park.[1] To increase the accuracy of a robotic manipulator, a visual-feedback control loop was used. They introduced the term of "visual servoing" to identify this type of systems. With this approach, a new field in robotics was opened, and since then a lot of work has been done in that direction. Visual servoing is the fusion of results coming from many elementary areas including high-speed image processing, kinematics, control theory, and real-time computing. An interesting work presented by Corke reviews this technique.[2]

* Dept. of Communication and Information Technologies, Polytechnical University of Cartagena (Spain).
† Dept. of System Engineering and Automatic Polytechnical University of Cartagena (Spain).
‡ U483 INSERM, IUT Cachan, Université Paris Sud, Cachan (France).

Later, approaches based on neural networks have been used to implement controllers for visual servoing systems.[3,4] These neural controllers note the positions of robots and objects, and can learn the relationship between robot joint angles and 3D position of the end-effector. Such systems have the drawback that they require training, but they give solutions for d.o.f. redundancy and eliminate the need for complex kinematic models of the visual-motor system.

Some researches of the CNS dept. at Boston University (USA) proposed several models of the sensory-motor control systems of the higher mammals.[5–10] These authors present a set of neural network models. Each of them performs a subtask, motivated by anatomical, physiological, and psychological data, in the larger task of visually guided reaching. The subtasks performed by these neural models are basically, the neural representation of a visually perceived target within a head-centered and body-centered coordinate frame, the formation of a spatial trajectory from a current hand position to the target, and the transformation of this spatial trajectory into joint angle commands (inverse kinematics). In Guerrero et al.[11–13] an original approach in this area was introduced. The authors considered the visual-motor problematic from a biological model transference. In these works, a control architecture, which implements these neural models to resolve the control problem of a robotic platform constituted by a robot arm and a stereohead, is proposed. This architecture tries to emulate the sensory-motor control system for the control of the arms. Basically, three modules constitute it: an internal representation of spatial positions, a controller for the stereohead and a controller for the robot arm.

One of the processes most studied in systems of robotic control based on tactile feedback has been the insertion of objects peg-in-hole. A classical control method has been used to grasp objects for insertion in 2D,[14–18] or in 3D with multifingered mechanisms.[16] In these cases some simple sensors incorporated in the fingers of a robot hand measure the force direction in each instance, in order to compensate for the movement of the robot hand. Gullapalli et al. presents an approach to the learning of the relationships between the contact forces measured with a six-axis sensor and the movements of a simple robot. The objective is to correct movements during an insertion task.[17] The proposed controller consists of a supervised neural net that calculates the gradient of the supervised evaluation parameter. The same method has been applied to the realization of more complex tasks (such as pick and place, active exploration

https://doi.org/10.1017/S0263574701003642 Published online by Cambridge University Press

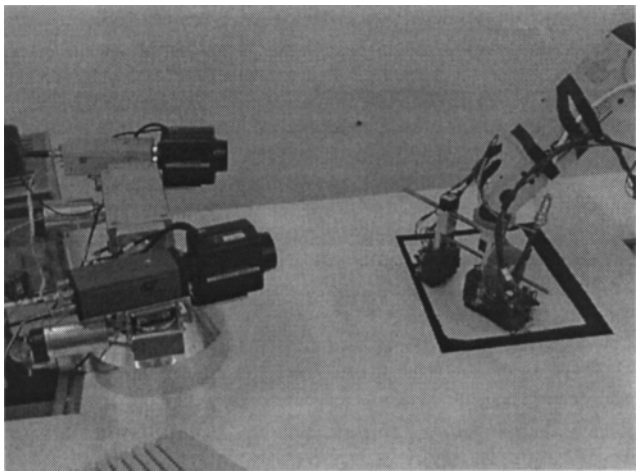


Fig. 1. Robotic Installation.



Fig. 2. LINCE stereohead.

and rotation of an object) with the UTAH/MIT robotic hand.[18]

A development of the Gullapalli et al. researches has been proposed by Cervera to implement a controller based on an unsupervised neural net of Self-Organizing Map (SOM) type.[19] It learns a map of the different states of contact in an insertion operation in 2D and as in flexible manufacturing systems. It is a function of the force signals obtained by a sensor attached to the upper face of the peg. This model guides the process with the minimal number of steps under conditions of uncertainty and a fixed number of functional class states of the contact situations.

Pedreño et al. described a sensory-motor control system constituted by a robot arm and two-finger gripper with artificial two tactile skins.[20] The authors developed a neural controller based on VAM (Vector Associative Map) algorithms. VAM algorithms initially proposed by Gaudiano and Grossberg,[21] allows to learn the transformations between the sensorial representations and the motor actions. The learning process is based on circular reaction concepts introduced by J. Piaget.[22] The neural controller proposed by Pedreño and collaborators, generates motor actions to position the force center detected on a tactile skin in a point of this surface. In their experiments the selected point was the center of the tactile surface.

In this work, a new approach in the visual-tactile-motor problem is presented. The control architecture proposed gives a solution for grasping hard object with the integration of visual and tactile information. The neural controllers implemented are based on the VAM algorithm, which permit one to project the retinal information of the cameras or the tactile information of the tactile skins over the joint space of the robot. The controller gives priority to the tactile information to guide visually the robot arm till the proximity of the objective. Then, the controller searches for a tactile stimulus. When the tactile skins detect forces, the controller takes into account only the commands of the tactile module.

This paper is organized in eight sections taking into account this introduction. Section II describes the principal parts of the robotic installation. Section III explains the structure of the VAM algorithm coordination in robotic reaching tasks. Section IV shows shortly the adaptation capability of the method. Section V and Section VI present respectively, the visual-motor controller and the tactile-motor controller. Section VII gives some experimental results and, Section VIII presents conclusions.

Table I. Characteristics of the stereohead.

	Convergence angles	Elevations	Panoramic
Range	±30°	±60°	±180°
Maximum Velocity	600°/sec	400°/sec	230°/sec
Maximum acceleration	6000°/sec	4000°/sec	1500°/sec
Actuator	DC Motor	DC Motor	AC Motor
Resolution	0.0045°	0.0036°	0.0018°
Base Line	360mm		
Weight	8.5 Kg		

2. ROBOTIC INSTALLATION

A robotic platform able to implement techniques of visual reaching has been developed. Three devices compose this platform: a stereohead, a gripper and a robot arm. Figure l shows the arrangement.

The robot arm is a CRS commercial device with five degrees of freedom. Three of them are dedicated to the positioning (base, shoulder and elbow) and two for the end-

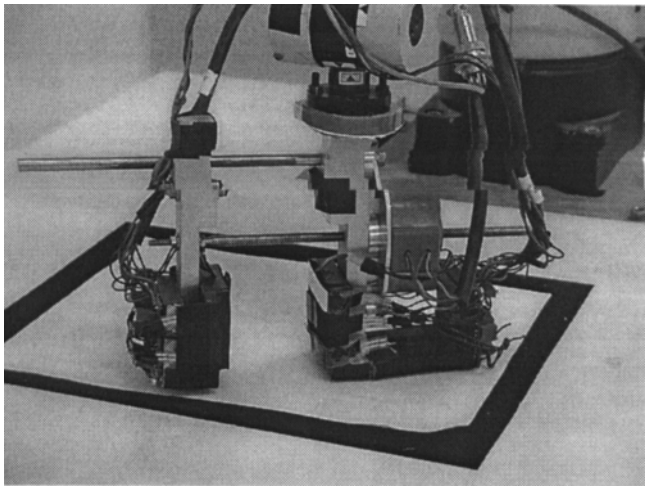


Fig. 3. Tactile skins in a two finger gripper.

https://doi.org/10.1017/S0263574701003642 Published online by Cambridge University Press

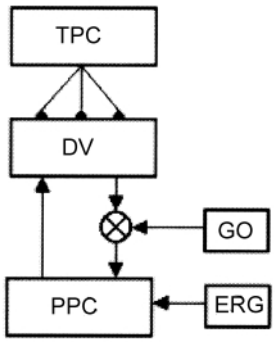


Fig. 4. VAM algorithm scheme.

effector (wrist angle and wrist rotation). A custom made controller has been designed by our group, to enhance the communication capabilities and fit for real-time applications.

For the visual perception a stereohead was used. This one is LINCE, which is a novel and high performance stereohead designed by our research group.[11] This visual robot device has five degrees of freedom (two vergences, two elevations and a panoramic joint). The stereohead was designed to include a motorized lens, with controllable focus, zoom and aperture. The actuators were arranged with the idea to achieve good resolutions of their joint movements, to reduce the gravitational and inertial effects, and to achieve a robust and compact mechanical device. The support of the cameras can be moved to make the optical center of the camera coincide with the elevation axis. These

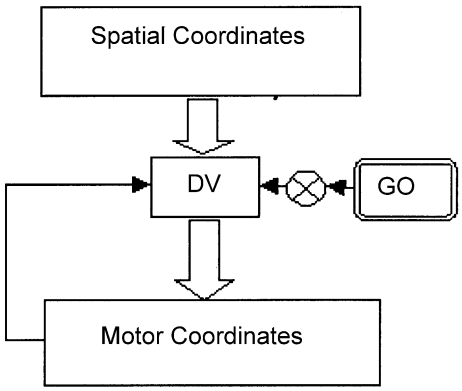


Fig. 5. Schematic diagram of the model.

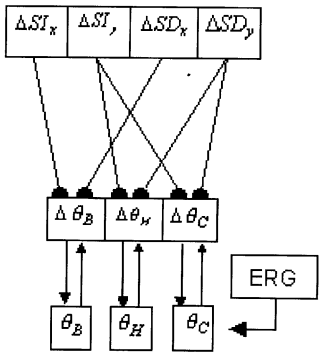


Fig. 6. Visual-motor neural model.

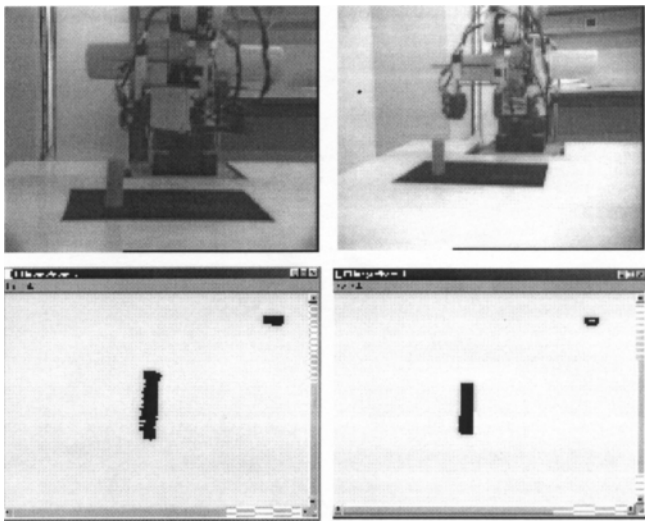


Fig. 7. Visual detection process.

adjustments permit the LINCE system to support different video cameras or laser pointers. Table I shows the main characteristics of our stereohead system.

The joint controller of the stereohead is a custom-made design. This hardware actuates over all the degrees of freedom of the stereohead system: five mechanical and four optical joints. The controller communicates by serial link to 30.400 baud through a packet-based protocol. This controller implements more than a hundred commands. These commands carry out different functions, as for example the change of the trajectory parameters or of the control algorithm parameters or to the synchronization of the different joint of the robot. Figure 2 shows the LINCE stereohead.

A robotic gripper with one degree of freedom was designed. This device incorporates two tactile surfaces with artificial tactile skins (Piezoresistive sensors; Interlink Electronics), located on both surfaces and covered by a rubber surface of 3 mm width. This elastic cover allows one to obtain a homogeneous distribution of the applied force. This effect is especially important for points on the surface edge. The dimensions of these surfaces and the path of the gripper allow the grasping of objects of different shapes.

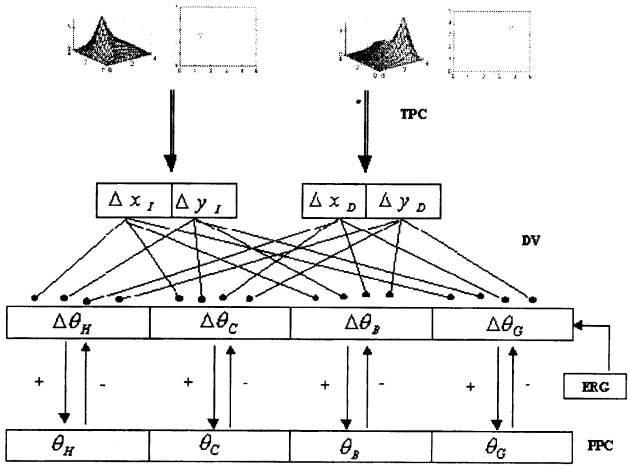


Fig. 8. Grasping VAM architecture.

https://doi.org/10.1017/S0263574701003642 Published online by Cambridge University Press

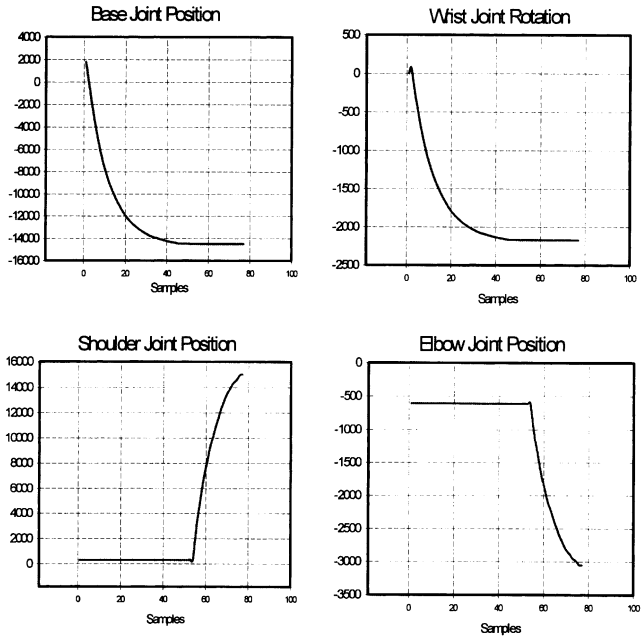


Fig. 9. Joint evolution of the robot arm in a reaching process for a determined value of the GO feedback signal.

Figure 3 shows a picture of the gripper with sensorial surfaces.

The actuation of these d.o.f. is made with a stepper motor coupled through a gearbox with a great reduction ratio, which increases the precision of the movements. The electronic controller of this device was integrated with the robot arm controller to enhance the robustness of the gripper-arm robotic set.

3. STRUCTURE OF THE NEURAL ALGORITHM

This controller implements a self-organized neural network with a VAM (Vector Associative Maps) structure, which has been developed in the CNS department of the Boston University. The VAM model is a general purpose model, not supervised, based on error and with real-time operation capabilities. Figure 4 presents a scheme of the implemented VAM algorithm.

The components of this model are as follows:

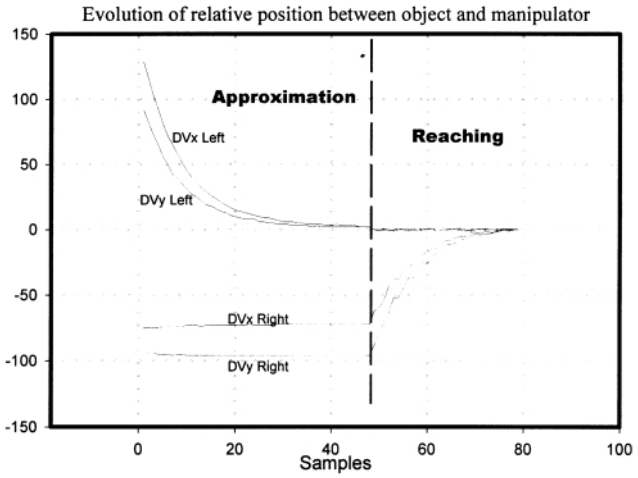


Fig. 10. Evolution of the relative position.

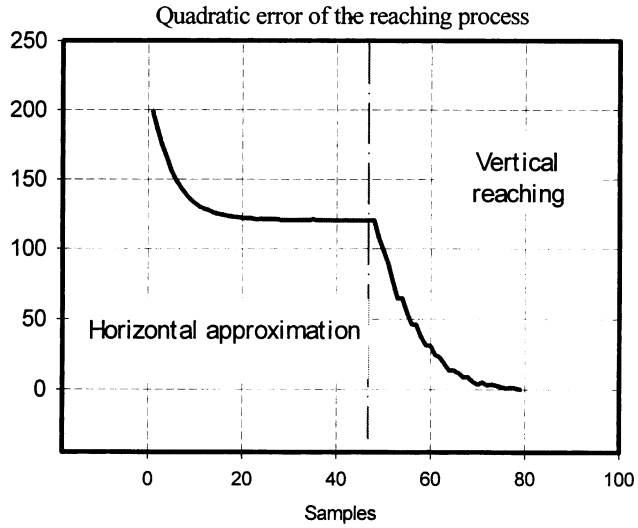


Fig. 11. Error evolution in the reaching process.

(i) *TPC*: Target Position Command. This vector contains the desired position of the end-effector in spatial map coordinates.

(ii) *PPC*: Present Position Command. This vector contains the actual position of the robot joints, in motor coordinates.

(iii) *DV*: Difference Vector. This vector computes the difference between the *TPC* and *PPC*.

(iv) *ERG*: Endogenous Random Generator. This module intervenes in the learning phase of the algorithm. The ERG module generates commands for joint positions.

3.1. Learning phase

The TPC block is connected to DV by means of adaptive neuron weights. It allows this model to work with representations of different type of data in the *TPC* and in the *PPC*. The learning process of adaptive connections is carried out by means of action-perception cycles in the ERG module.

The *DV* block adapts the matrix of neuron weights (Zij). It minimizes the produced error between the present position of the joints and estimated position while learning the transformation of coordinates. The matricial expression of increments in joint positions is as follows:

$$\begin{pmatrix} \Delta\theta_1 \\ \vdots \\ \vdots \\ \Delta\theta_N \end{pmatrix} = \begin{pmatrix} Z_{11} & Z_{12} & \dots & \vdots & Z_{1M} \\ \vdots & \vdots & \vdots & \dots & \vdots \\ \vdots & \vdots & \vdots & \dots & \vdots \\ Z_{N1} & Z_{N2} & \dots & \vdots & Z_{NM} \end{pmatrix} \times \begin{pmatrix} \Delta S_1 \\ \vdots \\ \vdots \\ \Delta S_m \end{pmatrix} \quad (1)$$

where:

$\Delta\vec{\theta}$: n joints positions of the robot arm.

$\Delta\vec{S}$: m sensorial inputs from the visual and tactile sensors.

It allows the association between the maps of the sensorial (visual and tactile) maps and the motor coordinates of the

https://doi.org/10.1017/S0263574701003642 Published online by Cambridge University Press

robot arm. Applying the least mean square method (LMS), the Z matrix is obtained at the end of the learning process, by evaluating the expression:

$$Z=(\Delta\vec{S}^{t}\times\Delta\vec{S})^{-1}\times\Delta\vec{S}^{t}\times\Delta\vec{\theta} \quad (2)$$

The end of the learning phase occurs when the variation of the weights reaches zero: $dz_{ij}/dt=0$.

3.2. Operation phase

Feedback allows to control the final position of the robot joints (Figure 5). The signal GO is a multiplicative gate that is able to control the velocity of the movement and the error evolution of DV.

This feedback model has the capability of indicating a new target, once the guided movement towards the initial object has been started. Thus, these problems based on the prediction of trajectories are avoided.

4. ADAPTATION CAPABILITY BASED ON ITERATIVE METHOD

After an initial learning process, as described above, the control system is able to learn each new reaching and grasping phases.

In this algorithm, the new values of the Z neural weights matrix tend towards the opposite direction of the quadratic error gradient. These values are calculated by the following iterative equation.

$$\frac{dZ_{ijK}}{dt}=\eta\cdot s_j\cdot\Delta h_i \quad (3)$$

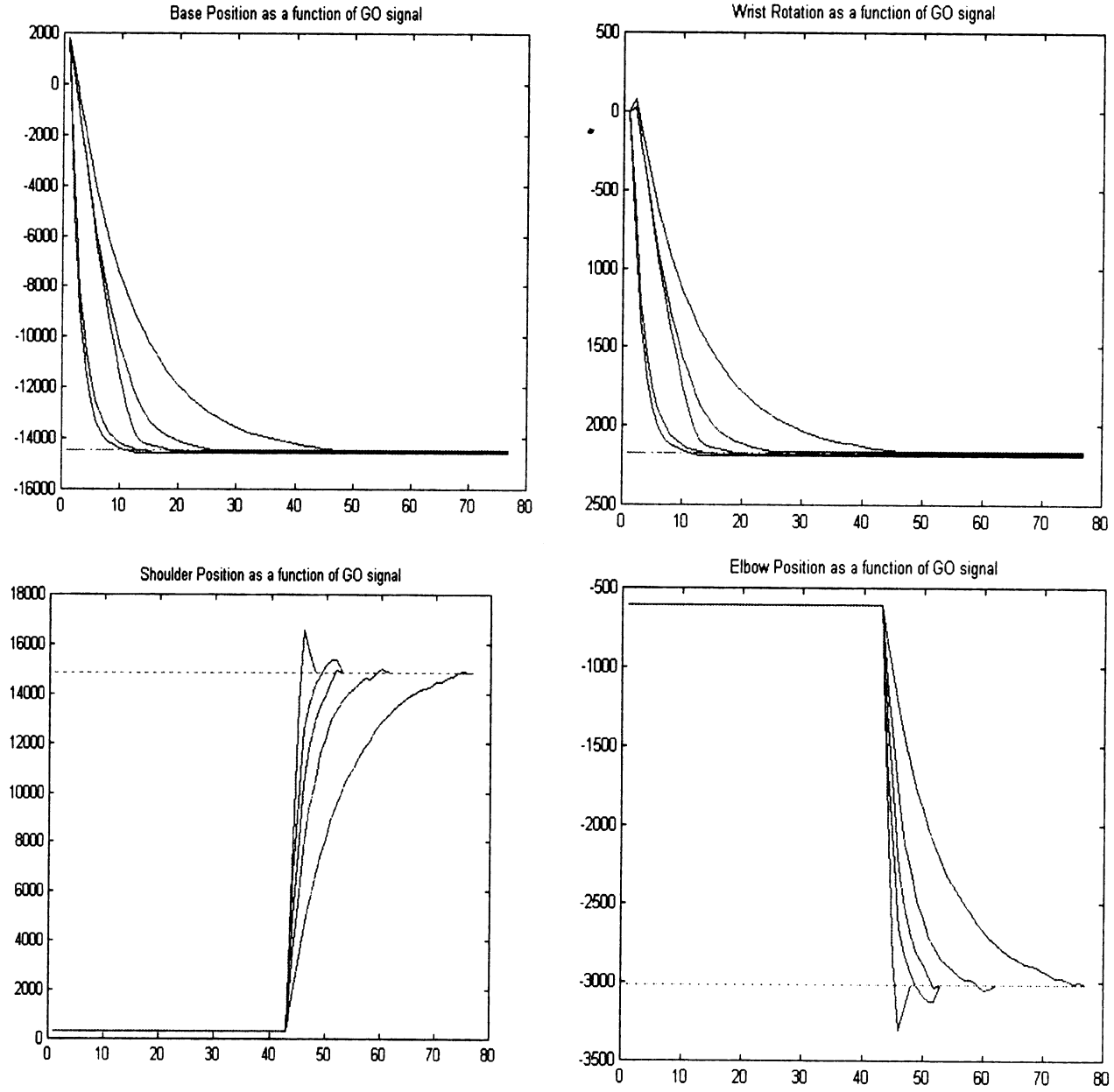


Fig. 12. Joint positions controlled by GO signals.

https://doi.org/10.1017/S0263574701003642 Published online by Cambridge University Press

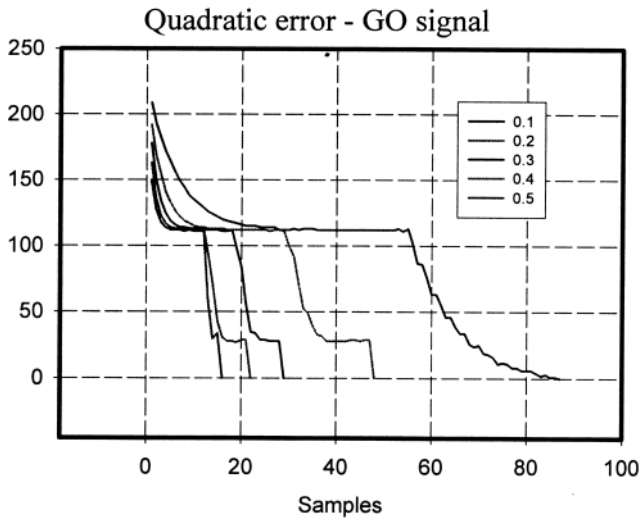


Fig. 13. Quadratic error for different GO signals.

where,

$$\Delta h_i = r_i - \sum_{j=1}^{M} Z_{jiK} \cdot s_j \qquad (4)$$

η: Learning rate
Vector r: motor positions [1 × n] (with n = number of robot joints).
Vector s: spatial positions [1 × m] (with m = number of sensorial inputs).
k is the number of samples.

In case of visual-motor and tactile-motor control these indices are, respectively, n = 3, m = 4 and n = 4, m = 4. The "η" parameter determines the speed of the iteration stability, in order to obtain an optimum convergence of the weights. Its value is so selected as to make the maximum increment of the Z matrix less than a threshold. While the system carries out new centered grasping, the error is minimized and the neural weights are changed more slowly.

This implemented algorithm allows the system to correctly behave when an unexpected event occurs (in some of the robot joints, stereohead joints, new sensorial elements in the tactile skins or visual detection).

5. VISUAL-MOTOR CONTROL FOR REACHING TASKS

When the control system is activated, the vision system detects the relative positions between the object and the manipulator. The three-dimensional coordinates are projected over the bi-dimensional reference system of the cameras of the stereohead. Figure 6 shows the VAM structure for the visual-motor control.

The visual control system carries out the detection process of the object and one rectangular mark in the manipulator. It is based on colour detection. The visual system computes in real-time the center of area of the object and a mark placed in the manipulator. In the learning phase, the algorithm establishes the relationship between the visual projections into the cameras and the joint positions (base, shoulder and elbow) of the robot arm.

In order to detect figures with minimum errors, the wrist angle of the robot arm turns towards an optimal angle of vision. Thus, the visual detection system measures with precision the relative position between the object and the manipulator by means of its projections. The object visual detection is shown in Figure 7.

The relationship between the wrist angle position and the base joint of the robot arm is defined according to the linear expression:

$$\theta_G = K \cdot \theta_B \qquad (5)$$

where the K parameter depends on the dimensions of the triangle formed by the two cameras and the initial base position of the robot arm.

The VAM neural controller will reduce the projective distance between these points and each camera to reach the end operation threshold. This operation is divided into two sequential phases: *horizontal approximation* and *vertical reaching*. In the first phase, the base joint is moved to reduce the distance of the x-axis projection of DV. In the second phase, the shoulder and elbow joints of the robot are moved to reduce the y-axis projection of DV. At the end of the operation, the object is between the two fingers. The

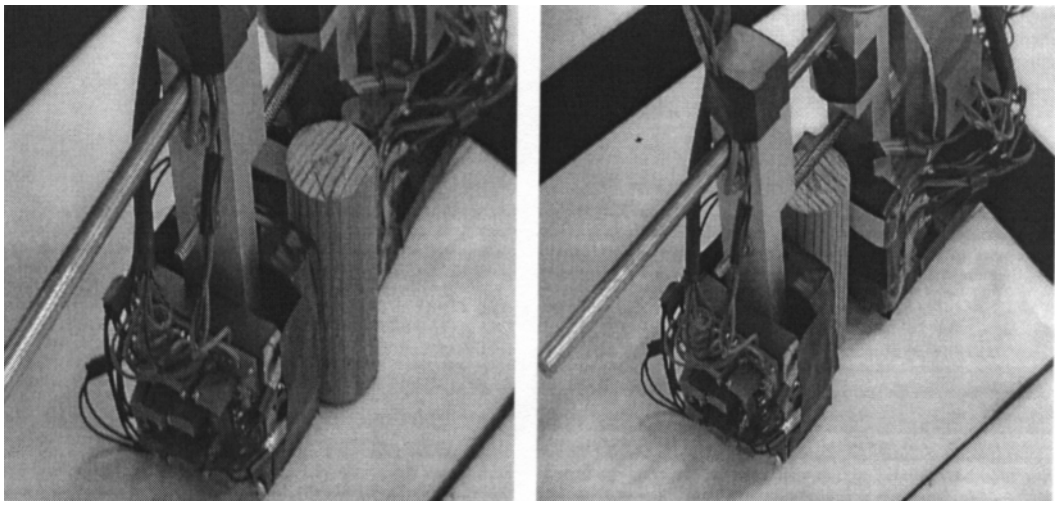


Fig. 14. Sequence of a grasping position correction.

https://doi.org/10.1017/S0263574701003642 Published online by Cambridge University Press

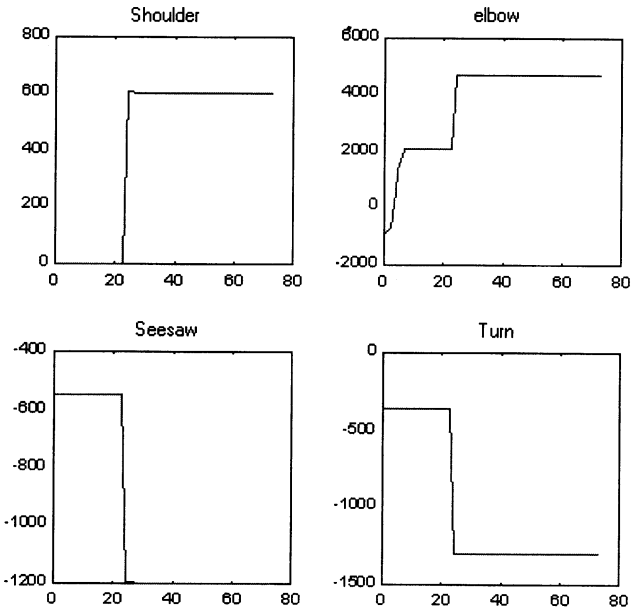


Fig. 15. Robotic joints evolutions.

grasping process will then center the object in the middle of the tactile surfaces.

6. NEURAL CONTROLLER FOR THE TACTILE-GUIDED GRASPING PROCESS

For the grasping control, the proposed VAM model guides the movements of the robotic arm and hand to grip an unknown object on the tactile surface center (Figure 8).

From the matricial feature, it is possible to obtain the sensory maps in grasping objects in real-time. Thus, the controller determines the centroids of the object in the surfaces by means of the obtained force distribution. The control system learns the directional mapping between the pressure distribution detected in the tactile skins when the system touches an object, and the joints' movements. Each movement implicates an increment of the localization of the centroids in the sensory surface tactile maps. Hence, the DV modifies the learning weights in order to lead these centroids to a selected position, in the actuation phase:

- **In the learning phase**, random increments are produced in the robot joints, which are related to the displacements of the tactile image centroids on the sensorial surfaces.
- **In the operation phase**, the algorithm computes the position of the tactile image centroids and moves the robot joints to center them over a selected cell of the artificial tactile skins. In order to increase the sensibility in the moment of the initial contact, a variable threshold in function of the phase grasping and manipulation, has been defined.

In this implementation, the neural controller moves the robot joints to position the centroids of the tactile images in the center of the tactile surface. This operation allows the application of the algorithm to any artificial tactile skin surface, independently of its shape. Therefore, this application may be generalized to any grasping robotic system.

7. EXPERIMENTAL RESULTS

To evaluate the performance of this algorithm, several robotic operations are analyzed with different objects (cylinders and spheres). The control problem is divided into three processes: *reaching*, stable *grasping* and *positioning* the object in a prefixed position.

Initially, the robot hand-arm and the object to be grasped are located in a random position over the platform. The wrist angle joint turns towards the optimal visual position in function of the arm base joint position. Then, the visual-guided reaching phase over the object minimizes the relative position between the object and manipulator (Figure 9).

First, the X axis approximation is produced, positioning the manipulator over the object. Next, the Y axis approximation locates the object between the two fingers of the robot manipulator, by means of the shoulder, elbow and wrist angle movement.

The GO parameter is selected to make the robot joints converge to the objective. The curves of Figure 10 represent the evolution of DV by means of the four visual projections.

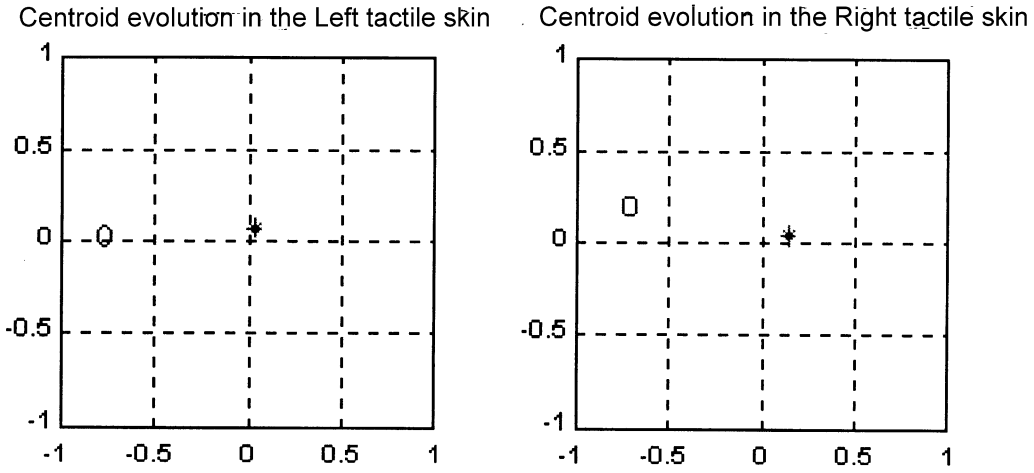


Fig. 16. Centroids evolution on tactile surfaces.

https://doi.org/10.1017/S0263574701003642 Published online by Cambridge University Press

Thus, it is clearly possible to distinguish the two phases of positioning and reaching.

The above curves correspond to the evolution of the error in horizontal projection for each camera. It tends to zero when the base joint position is nearby the object. Figure 11 represents the total mean quadratic error produced in both projections as a function of the sample time. This error is defined by the sum of the quadratic errors into the two spatial coordinates. The projections in left and right cameras in the "k" instant are represented by the vectors (X_{lk}, Y_{ik}) and (XD_k,YD_k).

The errors in the horizontal approximation and in the vertical reaching process are evaluated by the expressions:

$$\text{Error } X_k = \sqrt{XI_k^2 + XD_k^2} \tag{6}$$

$$\text{Error } Y_k = \sqrt{YI_k^2 + YD_k^2} \tag{7}$$

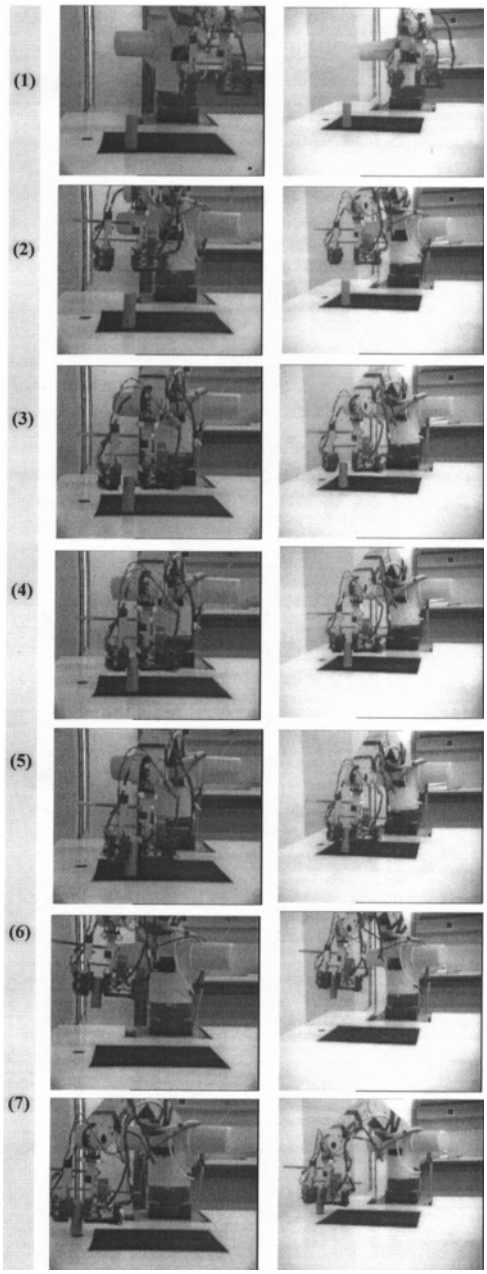


Fig. 17. Sequence of reaching and grasping.

The total error in both projections is:

$$\text{Error}_k = \sqrt{\text{Error } X_k^2 + \text{Error } Y_k^2} \tag{8}$$

The GO feedback parameter allows the system to control the velocity of the joints' position convergence. A low value of this parameter induces a low reaching error in both projections. However, the velocity of reaching will be small because the controller needs to take a lot of samples of visual images for a high feedback.

In the opposite case, a high value of this GO parameter will have an opposite effect. Besides, the velocity and the error of the reaching process are high. The small sampled velocity of the DV block produces oscillations with regard to the desired final position of the robot joints. Different values of the GO feedback parameter show the evolution of the robot joints (in Figure 12).

This study has determined an adequate value of GO parameter as 0.3. It satisfies the current conditions of robotic control: convergence, minimizing errors . . . The comparison of the error for each level of feedback is represented in Figure 13.

In this figure, the criterion for the selected GO value is clearly justified. The number of samples is a third of the signal that produces a minimal error.

After the reaching phase, the robot hand begins the gripping operation till the tactile images are centered on the surfaces. We have noticed that only one simple grasping positioning correction is necessary to center the tactile images on the sensorial surface. Each grasped object generates a force distribution map, which is the input information for the VAM controller.

When the tactile maps are obtained on the two sensorial surfaces, the algorithm computes the grasping forces. The joint increment to move the centered position to the center of the tactile surfaces is determined. These vectors are the feedback of the neural net. Hence, a grasping motion is produced to center the object in the artificial tactile skins. Figure 14 shows a sequence of complete grasping position corrections.

Figures 15 and 16 show the centroids evolution of the object center on the tactile surfaces and the joints evolution. Circle and star points indicate, respectively, the initial and final position of the centroid.

Finally, Figure 17 shows a complete sequence of reaching, grasping and pick-and-place operation.

Seven steps are required for reaching, grasping and moving the object in the final pick-and-place task.

In step (1), the robot arm and the object are located in a random position which belongs to the workspace of the vision system. The horizontal approximation of the arm robot is produced in *step (2)*. During the *Step (3)*, a vertical reaching process is produced. Along all the robot movements joints, the wrist angle orients itself towards the optimal position of the visual projection. In *step (4)*, the two fingers of gripper close around the object. When the object has been grasped, the controller computes the force distribution map. By means of the proposed neural algorithm, the controller moves in *step (5)* to lead the centered position towards the center of the tactile surfaces. Finally, in *step (6)* the system carries out a pick movement of the

https://doi.org/10.1017/S0263574701003642 Published online by Cambridge University Press

object and, then in *step (7)*, the object is placed in the prefixed position.

8. CONCLUSION

In this paper, the tactile-visual-motor integration problem is tackled by applying a neural VAM architecture to a robotic installation composed of a stereohead, robot hand-arm and artificial tactile skins. The algorithm proposed has produced good results in the reaching and stable grasping tasks of objects placed in random positions. The reaching process allows to position two fingers of the gripper around the object with a good response in term of velocity and errors. The grasping process insures the stability and the accuracy of the contact position. The adaptation capability of this model has presented a good behaviour of the system working under conditions of uncertainty. From the obtained results, the controller allows to grasp an object located in an unknown position and place it in a previous defined position whatever the robotic visual-tactile motor installation.

Acknowledgements

The authors would like to thank the Spanish Research Foundation (CICYT) for the support given to the project TIC99-0446-C02-01, and to the European Community for the support to the Brite Research Project SYNERAGH, ref. BRE-CT98-0797.

References

1. J. Hill and W.T. Park, "Real-time control of a robot with a mobile camera", *International Symposium on Industrial Robots* (1979), pp. 233–246.
2. P.I. Corke, *Visual Control of Robots: High Performance Visual Servoing* (Research Studies Press, John Wiley, 1996).
3. H. Hashimoto, T. Kubota, W.C. Lo, and F. Harshima, "A control scheme of visual servo control of robotic manipulators using artificial neural network", *Proc. of IEEE Int. Conf Control and Applications*, Jerusalem (1989), pp. 3–6
4. W.T. Miller, "Sensor-based control of robotic manipulators using a general learning algorithm", *IEEE Trans. Robotics and Automation* **3**(2), 157–165 (1987).
5. D. Bullock, S. Grossberg, F.H. Guenther, "Neural Network modeling of sensory-motor control in animals", **In**: *Advances in Motor Learning and Contro1* (H. Zelaznik, Ed.), Human Kinematics Press, Champaign, Illinois (1987), pp. 261–292.
6. F. Guenther and D.M. Barreca, "Neural Models for flexible control of redundant systems", **In**: *Self-organisation, Computational Maps, and Motor Control* (P.G. Morasso and Vittorio Sanguineh, Eds), Elsevier, North Holland, (1997), pp. 383–421.
7. D. Greve, S. Grossberg, F. Guenther and D. Bullock, "Neural representations for sensory-motor control, I: Head-centered 3-D target positions from opponent eye commands", *Acta Psychologica* **82**, 115–138 (1993).
8. S. Grossberg, F. Guenther, D. Bullock and D. Greve, "Neural Representations for Sensory-motor Control, II: Learning a Head Centered Visuomotor Representation of 3-D Target Position", *Neural Networks* **6**, 43–67 (1993).
9. F.H. Guenther, D. Bullock, D. Greve and S. Grossberg, "Neural Representations for Sensorimotor Control, III: Learning a Body-Centered Representation of a Three-Dimensional Target Position", *Journal of Cognitive Neuroscience* **6**(4), 341-358 (1994).
10. D. Bullock, S. Grossberg and F. Guenther, "A Self-Organizing Neural Model of Motor Equivalent Reaching and Tool Use by Multijoint Arm", *Journal of Cognitive Neuroscience* **5**(4), 408–435 (1993).
11. A. Guerrero, J.L. Coronado and F. Garcia-Cordova, "A neural network for target reaching with a robot arm using a stereohead", *Proc. of IEEE Int. Conf. on System, Man and Cybernetics*, Tokyo (l999), pp. 842–847.
12. A. Guerrero, J.L. Coronado and J. Feliu, "Neural control architecture for a stereohead with multi-degrees of freedom", *Proc. of IEEE Int. Conf on System, Man and Cybernetics*, Tokyo (1999), pp. 848–853.
13. J.L. Coronado and A. Guerrero, "A new application of the DIRECT neural model to the visual control of a robot", *Proc. of IEEE Int. Conf System, Man and Cybernetics*, Nashville, USA (2000), pp. 167–171.
14. B. Borovac, D. Seslija and S. Stankovski, "Soft sensored grippers in assembly process", *Proc. of IEEE Int. Conf. on Robotic and Automation* (1992), pp 1283–1288.
15. P. Gorce, P. Bidaud and M. Picard, "Design of an autonomous robot gripper", *Proc of 4th Int. Symposium on Robotics and Manufacturing, ISRAM '92*, San Diego, USA (1992), pp. 265–269.
16. P. Gorce, C. Villard and J. L. Fontaine, "Grasping coordination and optimal force distribution in multifingered mechanisms", *Robotica* **12**(2), Part 1, 243–251 (1994).
17. V. Gallupalli, R.A. Grupen and A.G. Barto, "Learning reactive admittance control", *Proc. of IEEE Int. Conf. on Robotics and Automation*, Mineappolis, USA (1996), pp. 1475–1480.
18. K. Souccar and R.A. Grupen, "Distributed motion control for multiple robotic manipulators", *Proc. of IEEE Int. Conf. on Robotics and Automation*, Minneapolis, USA (1996), pp. 3434–3439.
19. E. Cervera and A.P. Del Pobil, "A SOM-based sensing approach to robotic manipulation tasks", **In**: *Kohonen Maps* (E. Oja and S. Kaski, Eds), Elsevier Science B.V. (1999).
20. J.L. Pedreño-Molina, A. Guerrero-González and J. López-Coronado, "A Neural Controller for a Robotic Hand with Artifical Tactile Skins in Grasping Tasks", *Proc. of IEEE Int. Conf on System, Man and Cybernetics*, Nashville, USA (2000), pp. 161–165.
21. P. Gaudiano and S. Grossberg, "Vector Associative Maps: Unsupervised real-time error-based learning and control of movement trajectories", *Neural Networks* **4**, 147–183 (1991).
22. J. Piaget, *The Origin of Intelligence in Children* (International Universities Press, Norton, 1992) pp. 207–217.

https://doi.org/10.1017/S0263574701003642 Published online by Cambridge University Press